Creating Novel Sensorimotor Responses in Auditory Cortex

University of Oxford

Department of Physiology, Anatomy, and Genetics

MSc Neuroscience

Trinity Term 2019
Dissertation 2

Candidate Number
1030208

Word Count
8123

Supervisors
Samuel Picard Yves Weissenberger
Andrew King Johannes Dahmen

Abstract

Relating motor output to its sensory consequences is critical to navigating complex environments. In order to investigate the emergence of artificial sensorimotor contingencies, we trained mice on a novel sensorimotor task that required them to navigate through a virtual tonespace while recording from large numbers of neurons in auditory cortex using 2-photon imaging. Five out of nine mice learned the sensorimotor contingency and in an example session of one of those mice, a small proportion of neurons was sensitive to violations of the contingency. The task and its variations connect a simple behavioural paradigm in head fixed mice to some of the most debated computational theories of learning, producing neural and behavioural data that can be used to test their predictions.

Contents

1 | Introduction

Relating motor output to its sensory consequences is critical to simple movements and more complex behaviour. In the case of innate sensorimotor contingencies, the brain is thought to make use of corollary discharges, which cancel out the sensory consequence of a motor action by subtracting its predicted effect from the sensory input and play an important role even in simple circuits (Poulet and Hedwig, 2003). Whether they are mediated by elementary computations or require more finely tuned control, these corollary discharges demonstrate the existence and usefulness of a generative model of sensorimotor contingencies (Miall and Wolpert, 1996). These innate contingencies are also represented in sensory areas of the cortex where neurons signal the mismatch between visual input and predicted visual flow (Keller et al., 2012; Leinweber et al., 2017), and between vocalizations and auditory feedback (Eliades and Tsunada, 2018).

While the representation of innate sensorimotor contingencies is important for everyday behaviour, it is equally important to be able to recognize novel contingencies in dynamically changing environments. Humans and animals are adept at extracting statistical information from volatile environments (Behrens et al., 2007). This is mediated, in part, by sensory areas of the cortex, which are thought to construct a model of their environment (Berkes et al., 2011). In particular, some neurons respond more strongly to unexpected stimuli. For example, neurons in auditory cortex encode oddballs, tones that are unlikely according to the recent history of stimulus presentation (Gill et al., 2008; Rubin et al., 2016). This model guides how multisensory as well as sensorimotor information is integrated (Gallistel et al., 2001; Ernst and Banks, 2002; Körding et al., 2004; Körding and Wolpert, 2004).

In contrast to statistical patterns in the environment, artificial sensorimotor contingencies take the observer into account as a causal actor. Such contingencies are abundant in our daily lives, in particular in light of technological advancement, but it is advantageous for many animals to learn such novel rules, as well. Relatively little research has been carried out on this. However, Aronov et al. (2017) found that training rats to manipulate the frequency of a presented sound by pressing a lever resulted in the induced virtual tonespace being represented in a grid cell-like fashion in the hippocampal-entorhinal

circuit. Furthermore, it has been shown that neurons in auditory cortex suppress artificial sensory consequences of movement when mice are passively presented with such a contingency (Schneider et al., 2018).

In order to investigate the emergence of novel, behaviourally relevant sensorimotor contingencies, we trained mice to manipulate stimulus frequency by their licking behaviour while recording from large numbers of neurons in auditory cortex using 2-photon imaging. Mice were presented with tones at a regular interval and position in front of two spouts. Licking one of them led to a decrease in frequency of the presented tones, licking the other one led to an increase in frequency. In accordance with this contingency, the mice had to navigate to a rewarded frequency region in order to receive a drop of water. In this dissertation, I am going to investigate whether the mice were able to learn this task and what effect the presented contingency had on the activity of neurons in auditory cortex.

2 | Methods

2.1 Animals

2.1.1 Strain

All experiments were approved by the local ethical review committee at the University of Oxford and licensed by the UK home office. Eleven mice (three male (M01-03) and eight female (M04-11)) were used for the behavioural experiments. They came from a line obtained by crossing the floxed-Ai95 (RCL-GCaMP6f)-D line (Jackson Laboratories; stock number 024105) with the CaMKIIalpha-Cre T29-1 line (Jackson Laboratories; stock number: 005359). As a result, the mice expressed the fluorescent calcium indicator GCaMP6f (Chen et al., 2013) in cortical excitatory neurons.

2.1.2 Surgeries

At five to ten weeks of age, each animal was implanted with a metal head post and a cranial glass window over right auditory cortex, using surgical procedures described previously (Weissenberger et al., 2019). Briefly, after inducing general anaesthesia through the inhalation of isoflurane, the animal was placed in a stereotactic frame (Model 900LS, David Kopf Instruments). Body temperature and anaesthetic depth were monitored and kept constant throughout the surgery. The eyes were lubricated with eye ointment. Under aseptic conditions, the hair over the skull was removed. Following an incision into the scalp and the removal of the surrounding tissue, a 4mm circular craniotomy was drilled over right auditory cortex and a custom-made cylindrical window was placed onto the brain and glued to the surrounding skull. Post-operatively, the animals were given analgesia, kept warm, and monitored for at least 48 hours. All mice were allowed to recover for at least one week after surgery.

2.1.3 Preparations for behavioural training

After recovery, the mice were restricted to 1 ml of water per day in preparation of the behavioural training. Throughout the water restriction, the animal's weights were measured relative to their initial weight on a daily basis. Weight loss was kept constant around 85% and not allowed to fall under 80%. Behavioural training began after the weight had stabilized.

2.2 Materials

2.2.1 Behavioural setup

Mice M01-M07 were pre-trained in behavioural boxes before being imaged under the microscope, whereas mice M08-M11 were trained under the microscope setup from the beginning. For these purposes, several two-spout lick detection circuits were built following the diagram by Slotnick (2009). The mice were positioned in a conductive tube that was connected to this circuit. When they licked the spouts, which were also connected, they closed this circuit, which was registered.

In the behavioural boxes, the task was controlled using a custom-written program in Python 2 (Rossum, 1995) using the packages 'numpy' (Oliphant, 2006; van der Walt et al., 2011), 'random', 'time', 'multiprocessing', 'RPi.GPIO', 'csv', 'requests', 'pygame', and 'sys'. This program was executed on a Raspberry Pi 2 that was connected to the lick detection circuits and a solenoid responsible for delivering rewards in the form of 0.005ml drops of water.

In the microscope setup, the task was controlled using a custom-written program in Matlab 2017b (© Mathworks), which was connected to the task setup by a 10 MHz data acquisition board (National Instruments). This allowed for synchronization of the behavioural data with the microscope frame clock. Sound presentation was mediated using Psychtoolbox V3 (Brainard, 1997; Pelli, 1997; Kleiner et al., 2007). The levels of the presented sound were calibrated with a free-field high-frequency microphone (GRAS), and the latency of the sound presentation was determined and corrected for in the analysis.

Each animal performed the behavioural task once a day using between one and six blocks of training. Overall, this yielded 97 blocks of behavioural data from the box setup and 618 blocks of behavioural data from the microscope setup. Of these 618 blocks, imaging data was acquired on 233 blocks.

2.2.2 Two-photon imaging setup

Calcium imaging of auditory cortex was performed as described in Weissenberger et al. (2019), using a rotating two-photon laser-scanning microscope (Bergamo II, Thorlabs) with a 20x/1.00 immersion objective (Olympus). Excitation light (940 nm) was emitted from a femtosecond laser (Chameleon Discovery, Coherent) at 1250 mW, attenuated with a neutral density filter wheel (Thorlabs), and amplitude-modulated with a Pockels cell (302RM, Conoptics). This beam was then optically expanded and guided through a periscope into the scanhead where it was scanned onto the brain with an 8kHz resonant scanner and a galvanometric scan mirror, enabling the acquisition of 512x512 pixel frames at rates of 29.7 Hz. The microscope was controlled using ScanImage 2017 (Vidrio Technologies).

2.2.3 Widefield imaging setup

Widefield calcium imaging allowed for the identification of putative functional areas of auditory cortex. Before starting behavioural training, animals were head-fixed and passively exposed to a repeating sequence of eight different sinusoidally amplitude modulated (SAM) tones (4, 5, 25 & 32 kHz; 55 & 65 dB SPL; 500 ms duration; 10 Hz modulation frequency; 100% modulation depth; 15 repeats) . Images were acquired at 10 Hz through a TL2x-SAP objective (Thorlabs) and a 340M-GE camera (Thorlabs) using a blue LED for widefield excitation. Evoked responses to SAM tones were averaged (1-10 frames post-onset) and baseline corrected (1-6 frames pre-onset), and resulting response amplitude maps were plotted for each frequency-level combination. Based on the quality of the response maps, one pair of average low- and high-frequency SAM-responses was chosen for computing the widefield map. Two-photon images were registered to the widefield map by visually aligning the blood vessel pattern to the mean widefield image.

2.2.4 Imaging procedures

To record from neurons in the auditory cortex, the animals were head fixed in an optically and acoustically isolated imaging booth. During the subsequent imaging preparations, they performed the behavioural task. As a reference position, the microscope was positioned at the surface of the brain and the center of the widefield image. This allowed us to move the microscope to the functional areas of auditory cortex that had been identified using widefield calcium imaging and to find the same areas again across different days. Imaging was performed at planes of 170-250 µm below the surface, corresponding to cortical layers 2/3.

Subsequently, suitable areas for imaging were identified using the functional areas identified by the widefield image, the visibility of the neurons in these areas, and the robustness of their auditory responses. Several areas were recorded on different days to sample from different areas within auditory cortex. After selecting three to four locations in such a manner, these areas were repeatedly imaged throughout the remaining days as long as visibility allowed it. The same imaging location was determined using the reference frame and the brain surface, as well as a mean image of the recorded area to align the microscope between several days.

Imaging blocks of 10 minutes were acquired consecutively as long as the animal behaved sensibly, but never for longer than an hour. In this manner, imaging data were collected for 233 blocks, in total.

2.3 Behavioural paradigm

2.3.1 Sensorimotor task

The mice were head fixed in front of two spouts that were positioned either side of their snout. Sometimes the spouts were shifted to one side to counteract a bias into one direction. The mice were presented every 500 ms with pure tones that were 200 ms long and between 60 and 65 dB. These tones were centered around 11.3kHz and arranged in six steps per octave. When they were presented with stimuli spanning one octave, these were logarithmically arranged in the space between 8 and 16 kHz. A three octaves space spanned the range from 4 to 32 kHz. By licking the two spouts in front of them, the mice manipulated the frequency that was presented next. For this purpose, the counts nr and nl of right and left licks respectively were determined in either a window of 700 to 200ms or a window of 600 to 100ms before the next stimulus presentation. The current stimulus frequency was subsequently shifted by steps that were determined by rounding the formula

$$2\left(\log(n_r + 1) - \log(n_l + 1)\right)$$

to the nearest whole number. These shifts were bounded by the number of octaves in a given trial. Mice were presented either with an RL-contingency such that right licks led to a decreasing stimulus frequency and left licks led to an increasing frequency, or an LR-contingency, in which left and right licks led to decreasing and increasing frequencies, respectively.

When the tone frequency was at most one step away from the middle frequency (i. e. between 10 and 12kHz), mice were presented with a small drop of water (0.005ml) in the spout they had last licked.

In order to reach this rewarded region, the stimuli outside of this rewarded region therefore implied the strategy that needed to be employed in order to reach the rewarded region. In the RL-contingency (resp. LR-contingency), frequencies above (resp. below) the rewarded region implied a 'Rightwards!' strategy, where the animal needed to lick right, and frequencies below (resp. above) the rewarded region implied a 'Leftwards!' strategy, where the animal need to lick the left spout (see figure 3.1 for an example of an RL-contingency).

Recorded licks and rewards as well as presented sounds were registered in a text file for offline analysis.

2.3.2 Violations of the Contingency

For the purpose of understanding whether the mice had learned the sensorimotor contingency, and whether auditory cortex represented this contingency, targeted violations of the contingency were introduced to decouple sensorimotor dynamics from its confounding factors. When the lick rate was non-zero, random jumps in tone frequency were occasionally being presented, violating the sensorimotor contingency.

Larger jumps led to perturbations in strategy. Without such perturbations, a sound-driven policy would lead to a motor pattern of alternating left and right lick bouts. Such a policy would be indistinguishable from a policy based on a regular motor pattern switching between left and right lick bouts. After a strategy perturbation, an animal implementing a motor-driven policy should employ the same lick pattern as if the perturbation had not occurred, whereas an animal implementing a sound-driven policy should adapt its behaviour accordingly. By comparing the licking behaviour after such an event with the regular licking behaviour, a sound-driven policy could therefore be distinguished from a motor-driven policy. For this purpose, jumps were generate from a uniform distribution including all possible changes.

These large jumps were apparent as sensory oddballs. In the case of smaller jumps, the tones could be matched with tones following the regular contingency for their frequency and sound history (going back one stimulus). If the recorded neurons reacted differently to those tones violating the sensorimotor contingency, this would therefore indicate that these neurons represented the sensorimotor contingency. For this purpose, jumps were randomly generated from the prior distribution of stimulus changes.

2.3.3 Sound level modulations

Cortex has been demonstrated in multiple areas to integrate multimodal information according to their respective precision (Körding and Wolpert, 2004). In order to probe the integration of sensory and

motor evidence sound levels were decreased by 20 dB in some sessions to manipulate their precision. In these sessions, every stimulus had an equal probability of being represented at a sound level of 40-45 dB or 60-65 dB.

2.3.4 Training Methods

In the beginning, the mice were rewarded for licking the spouts to guide their behaviour into the correct direction. Subsequently, they were presented with a simple version of the behavioural paradigm, where the sounds were presented within one octave and without perturbations. As the animals' behaviour stabilized this window was extended to two and finally three octaves and strategy perturbations were introduced. To guide their behaviour in the initial stages, rewards were presented outside of the rewarded frequencies if either of the following conditions was satisfied: 1) the animal licked after having not licked for two minutes; 2) the animal licked in the direction that moved it closer to the rewarded frequency region after having not received a reward for ninety seconds. These rewards were omitted from the analysis.

2.3.5 Imaging procedures

To record from neurons in the auditory cortex, the animals were head fixed in an optically and acoustically isolated imaging booth. During the subsequent imaging preparations, they performed the behavioural task. As a reference position, the microscope was positioned at the surface of the brain and the center of the widefield image. This allowed us to move the microscope to the functional areas of auditory cortex that had been identified using widefield calcium imaging and to find the same areas again across different days. Imaging was performed at planes of 170-250 µm below the surface, corresponding to cortical layers 2/3.

Subsequently, suitable areas for imaging were identified using the functional areas identified by the widefield image, the visibility of the neurons in these areas, and the robustness of their auditory responses. Several areas were recorded on different days to sample from different areas within auditory cortex. After selecting three to four locations in such a manner, these areas were repeatedly imaged throughout the remaining days as long as visibility allowed it. The same imaging location was determined using the reference frame and the brain surface, as well as a mean image of the recorded area to align the microscope between several days.

Imaging blocks of 10 minutes were acquired consecutively as long as the animal behaved sensibly, but never for longer than an hour. In this manner, imaging data were collected for 233 blocks, in total.

2.4 Reproducibility

The collected behavioural and neural data is available in the Python package 'toneworld', which was created for the purpose of this dissertation and also contains the behavioural and neural analysis pipeline. A small showcase of its functionality can be found in the appendix. The package relied on the packages 'copy', 'numpy', 'pandas' (McKinney, 2010), 'setuptools', 'tqdm', 'math', 'scipy' (Jones et al., 2019), 'bootstrapped', and 'plotnine'. Parts of the analysis specific to this dissertation were conducted in R (R Core Team, 2018) using the packages 'broom' (Robinson and Hayes, 2018), 'dplyr' (Wickham et al., 2019b), 'feather' (Wickham, 2019a), 'ggplot2' (Wickham et al., 2019a), 'grid', 'lubridate' (Spinu et al., 2018), 'magrittr' (Bache and Wickham, 2014), 'muStat' (Wittkowski and Song, 2012), 'png' (Urbanek, 2013), 'reticulate' (Ushey et al., 2019), 'stringr' (Wickham, 2019b), and 'tidyr' (Wickham and Henry, 2018). The dissertation itself was written in R using 'bookdown' (Xie, 2018), 'knitr' (Xie, 2019), and 'rmarkdown' (Allaire et al., 2019). The package and the code necessary to reproduce the dissertation is available upon request.

2.5 Behavioural analysis

In order to analyze the mice's behaviour, the lickrates before and after certain sound events were determined. For this purpose, only changing sounds were included to omit behaviorally inactive phases. When a sound changed from a frequency region that suggested one particular strategy to a region that suggested another strategy, this warranted a change in licking behaviour according to a sound-driven policy. Using bins of 250 ms, the average lickrates in a five second window before and after such a strategy event were therefore assessed.

Subsequently, the effect of strategy perturbations was analysed by comparing violations of the paradigm that led to perturbations to those that did not. Mann-Whitney U tests (Hodges and Lehmann, 1956) were used to assess the nully hypothesis that the lick rate either did not change or changed into the wrong direction.

This analysis was summed up by determining the change in lickrate difference induced by the sound events. For this purpose, the difference between the right and left lick rate in the second before and after stimulus onset was determined. The lickrate difference before stimulus onset was then subtracted from the lick rate difference after onset. A positive (resp. negative) change in lick rate difference thus implied that the corresponding sound event led to a higher proportion of right (resp. left) licks.

The Prentice-Wittkowski test (Prentice and Pyke, 1979; Wittkowski, 2007) is a generalization of the Wilcoxon rank-sum test that allows for between-group comparisons within blocks of unequal length. This test was used to assess the null hypothesis that in a random stimulus event, the change in lickrate difference was not positive where it should be positive and not negative where it should be negative. Events were blocked according to the day, and the previous strategy. The p-value was then determined for each mouse individually.

The course of behavioural learning in mouse M10 was first assessed by comparing the reactions to strategy perturbations on days one to seven to the reactions on days fourteen to twenty using the framework involving the Mann-Whitney U test and the Prentice-Wittkowski test described above.

Behavioural analysis was restricted to the sessions under the imaging setup. Due to a damaged headbar, mouse M05 could not continue its behavioural training in this environment. Behavioural data of mouse M02 suggested that the data collection had been corrupted. Both animals were therefore excluded from analysis. Including the corrupted data from M02 did not change the results of the Prentice-Wittkowski test across all animals.

2.6 Neural Analysis

The Suite2p package (Pachitariu et al., 2017) was used to preprocess the neural data, extract fluorescence traces and infer spike rates. Preprocessing involved registration of the image frames to a 100-frame mean image using efficient subpixel registration methods (Guizar-Sicairos et al., 2008), SVD decomposition and region of interest (ROI) detection. A classifier was used to select neurons from the candidate ROIs. The default classifier for this purpose was fine tuned by manual assessment for the first few sessions, considerably improving its performance. Finally, the spike-rates of these neurons were determined using the OASIS algorithm implemented in suite2p. This included classifying which of these regions of interest corresponded to actual neurons. The classifier for this purpose was fine tuned by manual assessment for the first few sessions and improved its performance based on these data. Finally, the spike-rates of these neurons were determined using the deconvolution algorithm included in 'suite2p'.

The auditory response of these neurons was determined by determining their spike-rate for the different tone frequencies in the 300 ms after stimulus onset. Since the stimulus lasted for 200 ms, this spike-rate included both onset and offset responses. Due to sensory adaptation, neurons generally react more strongly to changing stimuli (Westerman and Smith, 1984). For this reason, only changing tones were included in this analysis. Using a Kruskal-Wallis-test, a nonparametric analysis of variance (Kruskal

and Wallis, 1952), neurons were identified whose responses significantly differed across the presented frequencies ($p < 0.0001$). Only these neurons were included in the subsequent analysis. The best frequency was determined as the frequency that, on average, elicited the highest spike-rate.

As a next step, a Prentice-Wittkowski test was used to determine whether compared to regular sounds, the neural response significantly differed for events that violated the sensorimotor contingency, but were matched in the manner described above. This was first assessed on a population response, resulting in a single p-value. As a next step, this test was applied to every single neuron, resulting in a distribution of p-values. By shuffling the perturbations across events, the distribution of these p-values was determined under the null hypothesis that pure sensorimotor perturbations did not elicit different spike-rates in any neuron and compared to the true distribution of p-values.

3 | Results

3.1 Acquisition

This section discusses the behavioural evidence that the mice have learned the sensorimotor contingency. For the purpose of this analysis, this is assumed to be the case if the mice adapt their behaviour in a sensible and sound-driven manner, i. e. animals should lick in a manner that would bring the presented stimulus closer to the rewarded region. In particular, it is not sufficient if their behaviour can be explained by a behavioural policy that is based on a regular motor pattern that is independent of the sounds. It is possible to distinguish a sound-driven policy from such a motor-driven policy using the two groups of stimuli presented below. Based on these groups and focussing on mouse M10, the subsequent sections will discuss the acquisition of the contingency in all animals and the course of learning in M10 alone.

3.1.1 Distinguishing a sound-driven policy from a motor-driven policy

The following paragraphs are going to explain how targeted variations of the task paradigm can distinguish a sound-driven policy from a policy based on learned motor patterns.

At any given time, the spout the animal should lick is determined by the sounds the animal is hearing. In the excerpt shown in figure 3.1, initially the sounds are above the rewarded region, therefore the animal must lick right in order to reach the rewarded region. (Henceforth, such stimuli are called 'Rightwards!' sounds.) As the animal employs the correct strategy and licks right, it reaches the rewarded region and is thus presented with a drop of water. As it keeps licking the right spout, the correct strategy changes to 'Leftwards!'. The mouse switches its lick pattern and is therefore rewarded. Subsequently, the stimulus again changes to a 'Rightwards!' sound.

Based on the above reasoning we can assess whether the animal's behaviour is compatible with a

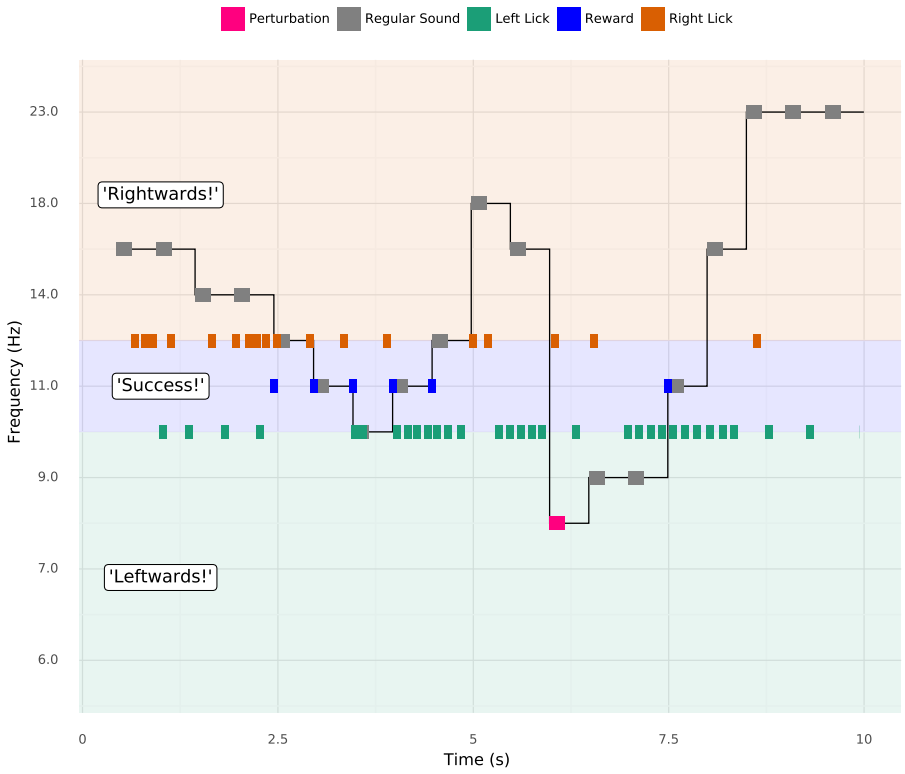

Figure 3.1: An example sequence of M10 undergoing the behavioural task. The gray tiles visualize the unperturbed presented stimuli. The time of stimulus presentation is shown on the x axis and their frequency in kHz is shown on the y axis. Pink tiles illustrate a perturbed sound. Furthermore, green tiles indicate left licks, orange tiles indicate right licks. Blue tiles indicate rewards.

sound-driven policy. In the example sequence, this is the case so far. However, it is not clear from this analysis alone that the changing sounds actually determine the lick strategy. Instead, the mouse might have learned a simple motor pattern of alternating between left and right lick bouts (henceforth called a switch policy). An animal simply switching between left and right licking independently of the sounds could nevertheless be regularly traversing the target region and therefore receive plenty of rewards.

By introducing targeted violations of the sensorimotor contingency, it was possible to analyse whether a switch policy alone could account for the behaviour. In some cases, such a violation led to a 'strategy perturbation', as can be seen in figure 3.1. By licking left, the animal had reached a 'Rightwards!' stimulus. Both a sound-driven and a motor-driven policy would suggest to lick right. However, due to a strategy perturbation, the stimulus suddenly jumps to a 'Leftwards!' sound, even though the normal sensorimotor contingency would have led to a 'Rightwards!' sound. The motor-driven policy would therefore erroneously suggest to switch and lick right, whereas a sound-driven policy would correctly suggest to not switch and continue to lick left. Strategy perturbations can therefore be used to distinguish between a switch policy and a sound-driven policy.

Of course, a different motor-driven policy could cause the mouse to correctly react to strategy perturbations, namely by continuously licking on one side. However, this policy would fail to provide the mouse with any rewards when no perturbations occur. Only a sound-driven strategy can account for the correct lick pattern in both cases. By comparing the effect of violations that lead to a strategy perturbation to those that do not, it is therefore possible to assess whether the mice have learned the sensorimotor contingency.

3.1.2 Lickrates after a strategy change

For the purpose of such a comparison, this section will analyze lickrates before and after sounds that imply a change in strategy, as well as before and after strategy perturbations, using M10 as an example. It is important to note that this mouse (like most others) was generally more likely to lick the left than the right spout.[1]

As figure 3.2 demonstrates in the case of mouse M10, a change in strategy is preceded by licking of the opposite spout, as this drives the sound into the corresponding region. Furthermore, it is followed by an increased lick rate in the direction that is suggested by the stimulus. This increase is pronounced for a 'Leftwards!' event and more attenuated – but nonetheless present – in the case of a 'Rightwards!'

[1] The consistent left bias might be explained by the position of the headbar and the cranial window that was also consistent across all animals. The added weight of these implants require compensatory mechanisms by the animals that might have induced the bias as a side effect.

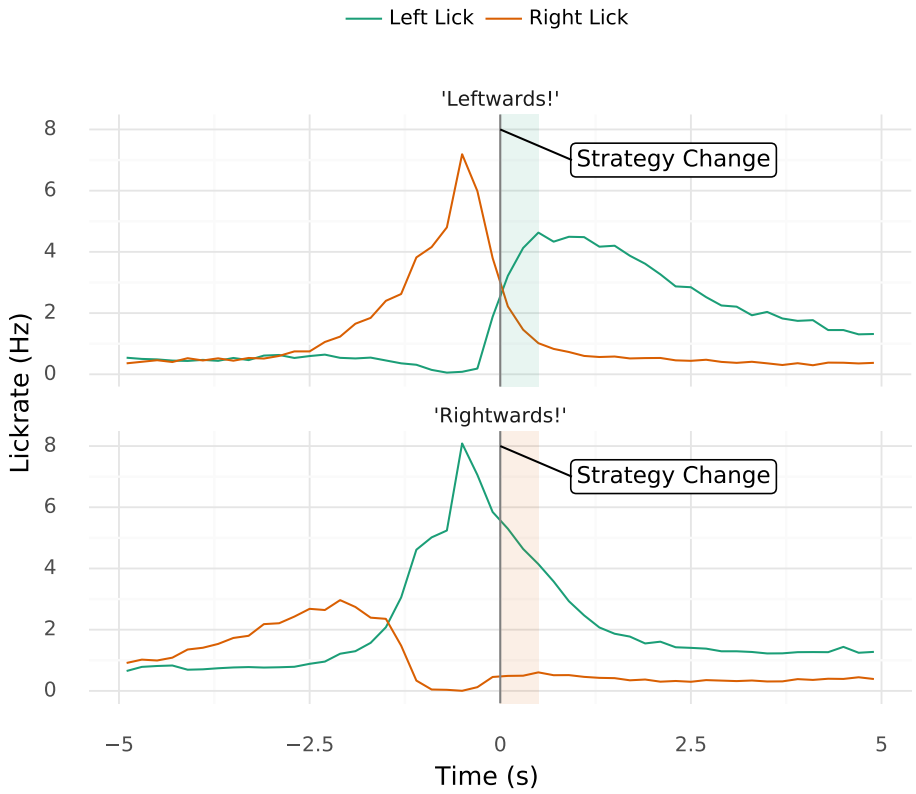

Figure 3.2: The lick rate before and after a sound that changes the appropriate strategy either to 'Leftwards!' (upper panel) or 'Rightwards!' (lower panel). Data has been averaged across all sessions by M10.

event. It begins about 500 ms before the sound that causes a strategy change and reaches its peak within 500 ms after that sound.

The animal therefore reacted to a strategy change in the appropriate manner. This reaction was either sound-driven or due to a learned switch pattern. In particular, this animal often started an active phase (i. e. a phase with a high lick rate) with a right lick bout that was followed by a left lick bout. In order to investigate whether such a motor pattern can explain away the animal's behaviour, figure 3.3 visualizes the average lick rates of M10 centered around violations of the contingency that either perturbed the current strategy (henceforth called 'perturbation' events, see figure 3.1) or did not perturb the current strategy ('no perturbation').

These violations only occurred during periods when the animals were actively engaged in the task, i.e. when the lick rate was non-zero in the immediate past, but were otherwise random. Restricting the analysis to those stimuli that represented a violation of the contingency therefore made the history between perturbation events and no-perturbation events comparable. As expected, the lick rates preceding stimulus onset were similar for both types. The only notable difference is given by an elevated right lick rate in the event of a 'Leftwards!' strategy without perturbation.

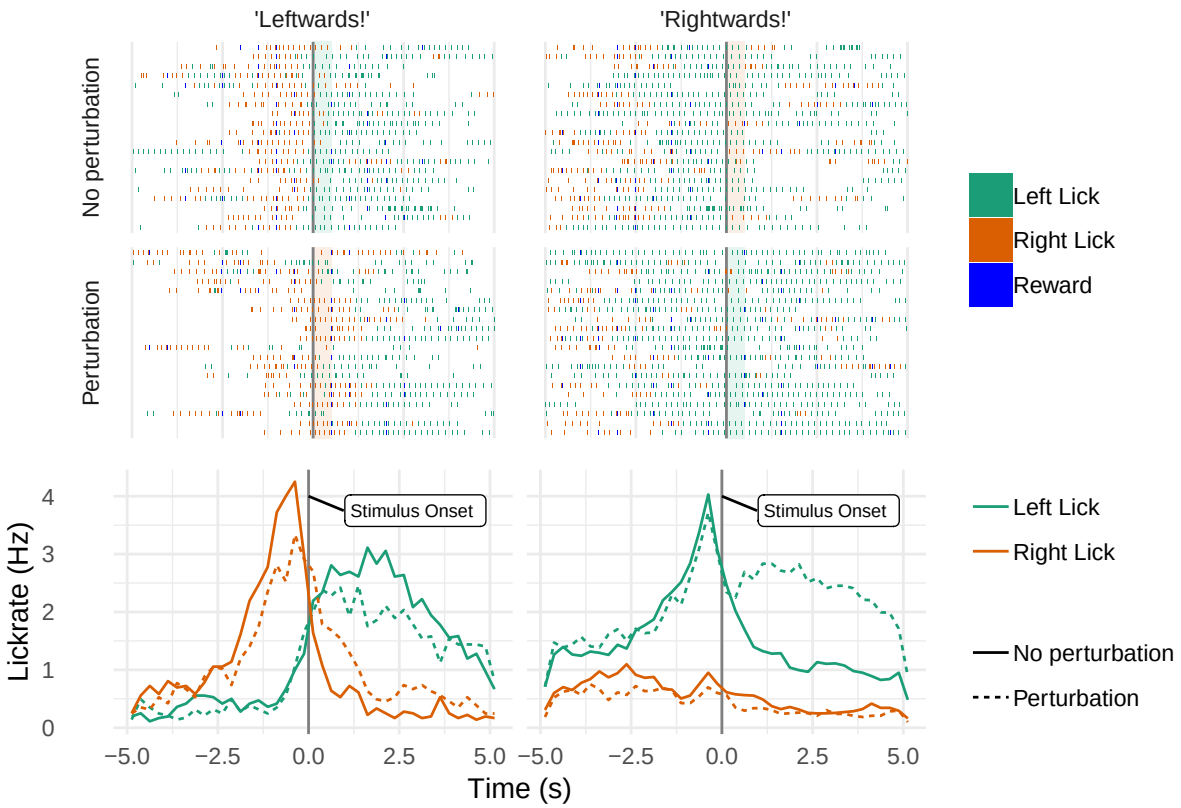

Figure 3.3: The top panel depicts, in a raster plot, example events centered around perturbed and unperturbed events. The bottom panel shows the lickrate histogram centered around these events for M10. The x axis shows the time centered around stimulus onset and the y axis shows the lickrate. On the left side, events where the sensorimotor contingency led to a 'Leftwards!' sound are depicted. In the no-perturbation case, the new sound still suggested a left lick bout. In the case of a perturbation event, the new sound suggested to lick right. On the right side, events where the sensorimotor contingency led to a 'Rightwards!' sound are depicted. Similarly, the no-perturbation case does not change this strategy, whereas the perturbation case does.

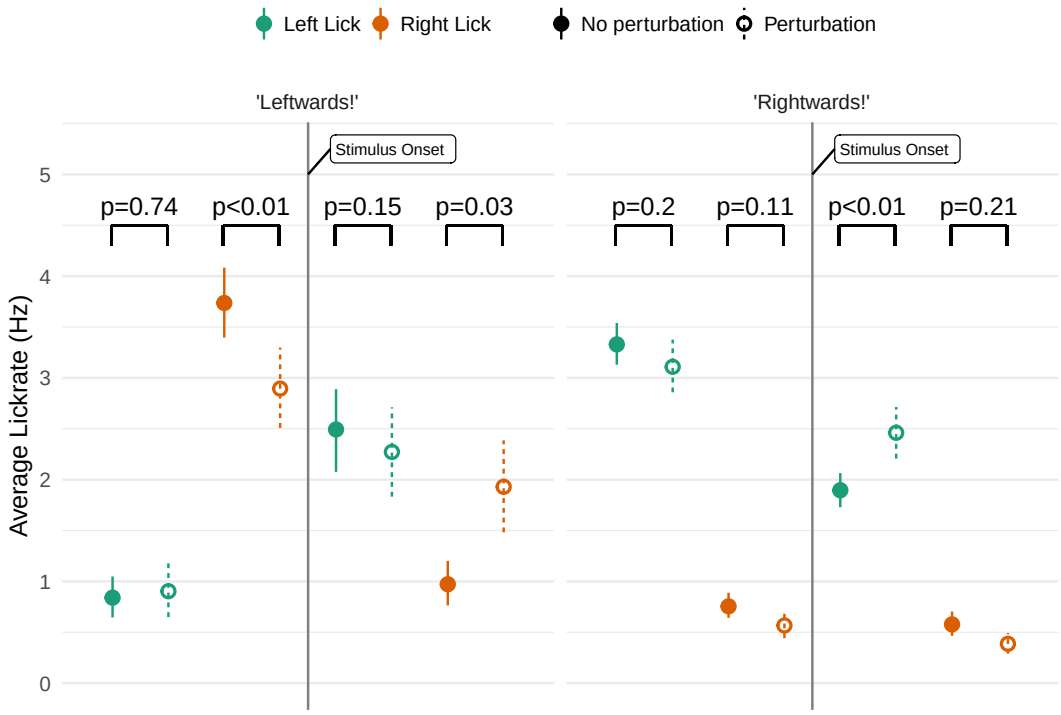

Figure 3.4: The differences in lickrates as a result of perturbation and no-perturbation events and the significance of their difference according to a Mann-Whitney U test.

The behavioural pattern following a no-perturbation event was consistent with the pattern following a strategy change within the sensorimotor contingency. In contrast, a perturbation of the strategy led to an immediate change of the left lickrate into the appropriate direction. If a 'Leftwards!' sound changed to a 'Rightwards!' sound, the left lick rate that had already started ramping up instantly decreased again. In the case of the reverse change, the left lick rate interrupted its quick decrease and instead increased again. Though less severely, the right lick rate changed in the appropriate manner, as well. The strategy perturbation therefore broke the regular switch pattern.

This response was not driven by random fluctuations. This could be confirmed by using a nonparametric test to compare the lick rates in the second before and after stimulus onset and comparing them between events that led to a strategy change and those that did not (see figure 3.4).In three out of four types of events, the licking behaviour of M10 before stimulus onset showed no significant differences between perturbation and no-perturbation events ($U = (8380, 95448, 105208)$, $p = (0.74, 0.20, 0.11)$). However, for a 'Leftwards!' strategy, right lick rates were significantly elevated in the event of perturbations compared to no perturbations ($U = 6418$, $p = 0.0025$).

In contrast, after a strategy perturbation, the lickrates into the direction of the perturbation significantly increased when compared to their level during a non-perturbed event in which licks into this direction were not necessary ($U = (9230, 111039)$, $p = (0.032, 0.0025)$). The lickrates into the

Table 3.1: Table summarizing the results of the Prentice-Wittkowski test for each mouse, specifying the result in terms of the test statistic χ^2 and the p-value.

Mouse	Test Statistic	p-value
M01	1.1000	0.86000
M03	0.0033	0.52000
M04	0.5700	0.23000
M06	9.5000	0.00100
M07	3.0000	0.04200
M08	6.5000	0.00530
M09	0.0021	0.48000
M10	13.0000	0.00012
M11	9.6000	0.00096

previous direction decreased in the event of a perturbation, but those changes were not significant ($U = (8814, 102516)$, $p = (0.15, 0.21)$).

These results demonstrate that lick strategies cannot be fully explained by a motor-driven policy, and are at least partly explained by a sound-driven policy. Therefore, we can conclude that M10 has acquired the sensorimotor contingency.

This analysis can be further summarized by determining and comparing the change in lick rate difference elicited by the different types of events. This change is defined as the difference between the right and left lick rate in the second after stimulus onset compared to the lick rate difference in the second before stimulus onset. A positive (resp. negative) change in lick rate difference therefore suggests that the proportion of right (resp. left) licks was higher following stimulus onset. Compared to regular sounds, strategy perturbations shifted this change in lick rate difference significantly into the correct direction in mouse M10 ($\chi^2 = 13.5$, $p = 0.00012$).

3.1.3 Group analysis of behavioural learning

The Prentice-Wittkowski test comparing changes in lickrate difference allowed for a compact assessment whether a mouse had learned the task using a sound-driven policy and indicated that five out of nine mice had learned to employ such a policy and therefore had acquired the contingency (see 3.1). The average reactions to a strategy perturbation can be found in the appendix.

3.1.4 Course of learning

In mouse M10, which performed this task for twenty days, this sound-driven policy emerges over the course of training. By splitting its sessions up into the first (days one to seven) and last (days fourteen

Figure 3.5: The top panels illustrate the differences in lickrates of M10 as a result of perturbation and no-perturbation events and the significance of their difference across the first seven days. The bottom panels illustrate that difference at the end of the behavioural training. The lineranges reflect 95% confidence intervals.

to twenty) third, it is possible to study the evolution of the sound-driven policy (figure 3.5).

The most important response to strategy perturbations, the increase of the lickrate in the appropriate direction, is not significant in the first seven days ($U = (1141, 8050)$, $p = (0.51, 0.91)$), but is in the last seven ($U = (764, 11090)$, $p = (0.03, 0.05)$). In contrast, the left lickrate is already significantly attenuated in the appropriate event within the first seven days ($U = 1450$,$p = 0.0080$).[2] In the last seven days, neither the right nor the left lickrate are significantly attenuated for perturbations that suggest a strategy in the opposite direction ($U = (544, 9512)$, $p = (0.80, 0.83)$). Overall, however, the behaviour of M10 can be better explained by a sound-driven policy for the last seven days compared to the first seven days, indicating an improvement in performance over time. This is supported by a Prentice-Wittkowski test applied to the first and the last seven days. While this test is significant in both cases, the test statistic is higher and the p value smaller at the end of the behavioural training (Days one to seven: $\chi^2 = 3.17$, $p = 0.038$; Days fourteen to twenty: $\chi = 20.8$, $p = 2.6e - 6$).

By assessing the change in lick rate difference that the four different kinds of strategy perturbations evoke on a daily basis, the emergence of the sensorimotor behaviour over time can be studied in

[2]It is important to note here that the first seven days contain few perturbations. This might be an explanation for the discrepancy between the overlapping confidence intervals and the significant Mann-Whitney U test, which evaluates a rank sum rather than a difference of means.

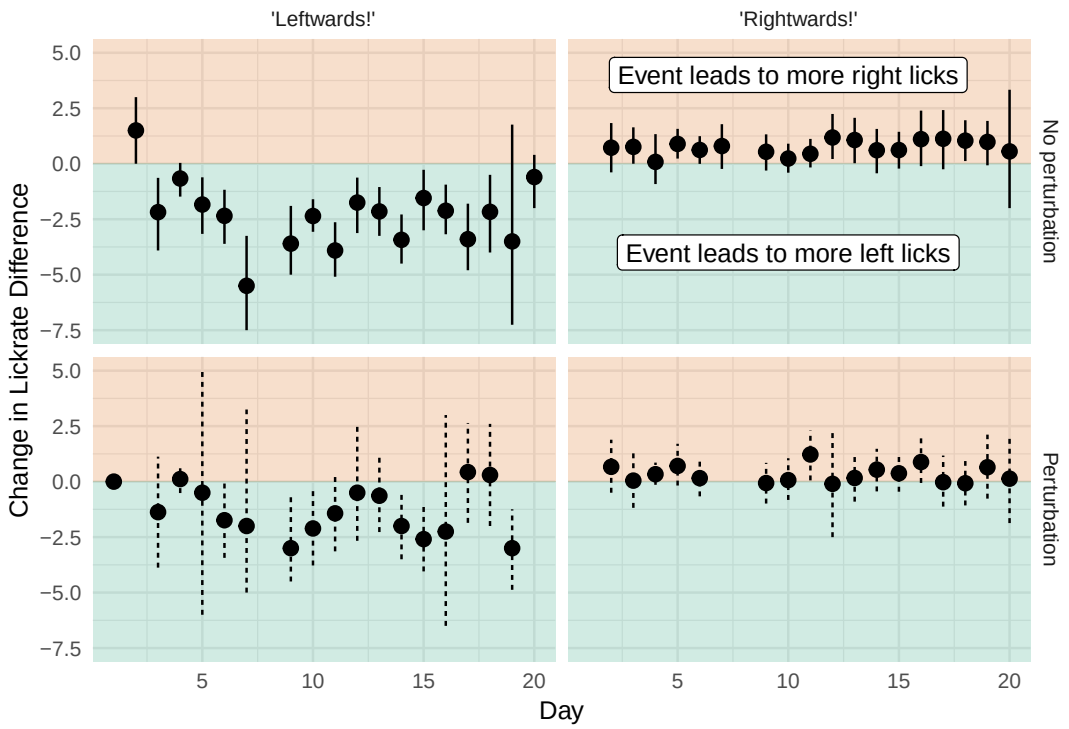

Figure 3.6: The evolution of the change in lick rate difference over training time.

a more detailed manner (figure 3.6). If the animal behaves in a sensible manner, this change in lick rate difference should be positive (resp. negative) if the sound suggests a 'Rightwards!' (resp. 'Leftwards!') strategy. Within the first couple of days, the change in lick rate difference in response to no-perturbation 'Leftwards!' events quickly reached a strong negative value. Compared to that the change in lick rate difference in response to no-perturbation 'Rightwards!' events rose more slowly. In a perturbed 'Leftwards!' event suggesting a right lick bout, the initial response appeared similar to a non-perturbed 'Leftwards!' event. Over time, however, compared to the regular reaction, this change in lick rate difference shifted towards a higher proportion of right licks. A similar, but more subtle pattern emerges from the perturbed 'Rightwards!' events, as well.

3.2 Representation

This section discusses the evidence that auditory cortex represents the sensorimotor contingency. For the purpose of this analysis, this is assumed to be the case if violating the sensorimotor contingency changes the representation of the presented stimulus. In the previous section, the contingency was violated with jumps large enough to induce a strategy change. Auditory cortex represents such sensory oddballs regardless of their relation to the contingency (Rubin et al., 2016). This analysis therefore required more subtle sensorimotor violations. To distinguish sensory oddball responses from sensori-

motor perturbation responses, events were selected that were matched in terms of sensory statistics, but differed from regular sounds in as far as they violated the sensorimotor contingency. Sensory statistics were assumed similar if the previously and currently presented stimuli were equal across both conditions.

If auditory cortex is sensitive to such subtle perturbations, this would therefore suggest that the area takes motor evidence into account in a contingency-specific manner. By recording single-neuron responses in auditory cortex while the mouse was engaged in the task and occasionally presented with perturbations, it was determined whether auditory cortex was sensitive to violations of the sensorimotor contingency.

3.2.1 Frequency tuned neurons in auditory cortex

As a first step, neurons were identified that were sensitive to the presented tones. In primary (A1) and secondary (A2) auditory cortex as well as the anterior auditory field (AAF), neurons are globally organized in a topographical manner according to their best frequency, i. e. the sound frequency they respond to most strongly (Stiebler et al., 1997; Bizley et al., 2005; Issa et al., 2014). Using widefield imaging, the location of the cranial window over auditory cortex was confirmed and the locations of A1, A2, and AAF were determined (figure 3.7a). While the mice performed the behavioural task, we recorded the activity from individual neurons in layer 2/3 (170-250µm depth) of these regions using 2-photon calcium imaging and determined the deconvolved spike rate using the 'suite2p' algorithm (Pachitariu et al., 2017). This section analyses an example session in L2/3 (-205µm) of putative A1 in mouse M10.

After determining the average spike rate in response to a presented stimulus, neuronal frequency tuning was determined using the Kruskal-Wallis statistic, a nonparametric version of the analysis of variance (Kruskal and Wallis, 1952). The neurons with the strongest frequency tuning ($p < 0.0001$) were selected for further analysis. Most of the selected neurons showed typical frequency tuning curves (figure 3.7b,c) and a typical average response to sound presentation (figure 3.7d), with a mixture of onset and offset responses (Qin et al., 2007; Liu et al., 2019).

3.2.2 Sensorimotor Perturbations

This section evaluates whether auditory cortex represents the sensorimotor contingency. This would be the case if the stimulus representation was different for sensorimotor perturbations compared to sounds that followed the contingency. In order to control for any neural effects driven by sound history

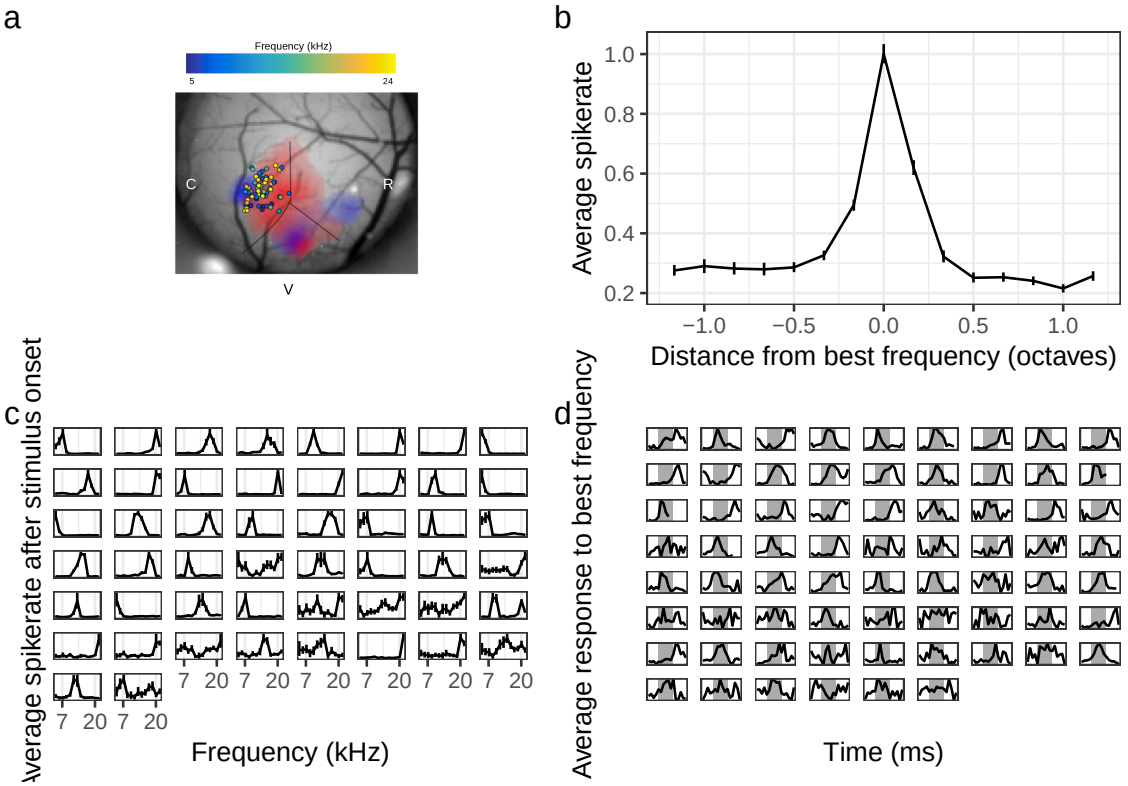

Figure 3.7: Frequency tuning in auditory cortex. **a** The recorded area in mouse M10. Shaded areas are pixels with significant responses (z-score> 1) to 4 kHz (blue) and 25 kHz (red) SAM tones. Putative boundaries between A1 (left), AAF (bottom), and A2 (right) are indicated. Frequency-tuned neurons are shown shaded according to their best frequency (kHz). **b** Average tuning curve centered around the best frequency of all neurons. Lines indicate 95% confidence intervals. **c** Tuning curves with 95% confidence intervals of the most strongly tuned neurons as measured by a Kruskal-Wallis test. Frequency varies along the x axis and spike rate varies along the y axis. The scale of the y axis is not consistent across neurons and has been omitted for clarity. **d** Average spike rates in response to a best-frequency stimulus presented for 200 ms (represented by the shaded block). Time varies along the x axis and spike rate varies along the y axis. Again, the scale of the y axis is not consistent across neurons and has been omitted for clarity.

statistics themselves, the responses to sensorimotor perturbations were compared to non-perturbed sounds with matched frequency and stimulus history (going back one stimulus).

A Prentice-Wittkowski test over the full population of frequency-tuned neurons revealed that the spike rates elicited by perturbed stimuli were significantly different from those following non-perturbed stimuli ($\chi^2 = 5.3$,$p = 0.02$). This suggests that the population of neurons recorded in this session indeed represents the sensorimotor contingency. Overall, the neurons appear more broadly tuned in the event of perturbed stimuli, though due to the limited sample size, this is difficult to assess using an averaged tuning curve (figure 3.8d).

Next, the representation of sensorimotor perturbations was considered at the level of individual neurons. Applying the Prentice-Wittkowski test to single neurons yielded nine out of 69 frequency-tuned neurons with a p value of under 0.05.[3] This was a higher number than what would have been expected due to random fluctuations: a permutation test with shuffled perturbations led to nine or more perturbation-sensitive neurons in less than 0.02% of the cases (i. e. p=0.0002) (figure 3.8b). This is further evidence that auditory cortex indeed represents sensorimotor perturbations.

Inspection of the neurons that were the most sensitive to perturbations reveals that in some cases, the perturbation modulated the amplitude of the neuronal response without affecting the frequency tuning, whereas in other cases, the response to sensorimotor perturbations was shifted in frequency. Figure 3.8e visualizes the average response to a best-frequency stimulus that represents or does not represent a perturbation. In many cases, the perturbation modulates the response, either by making it stronger or weaker. However, other effects can be found as well. In particular, one example neuron showed a broader frequency tuning to sensorimotor perturbations (figure 3.8f). Indeed, it was particularly sensitive to events whose expected sound was near the best-frequency stimulus, suggesting that it responded to a mixture of the presented and expected sound.

In this manner, inspection of single neurons can shed light on possible mechanisms by which sensorimotor perturbations are represented. The analysis presented here does not allow us to validate or reject such hypothesized mechanisms. At this stage, however, it is possible to confirm that neurons in auditory cortex represented, in some way, sensorimotor perturbations differently from sounds within the contingency.

[3]Note that on a neuronal level, the test has much less statistical power due to the strongly reduced sample size.

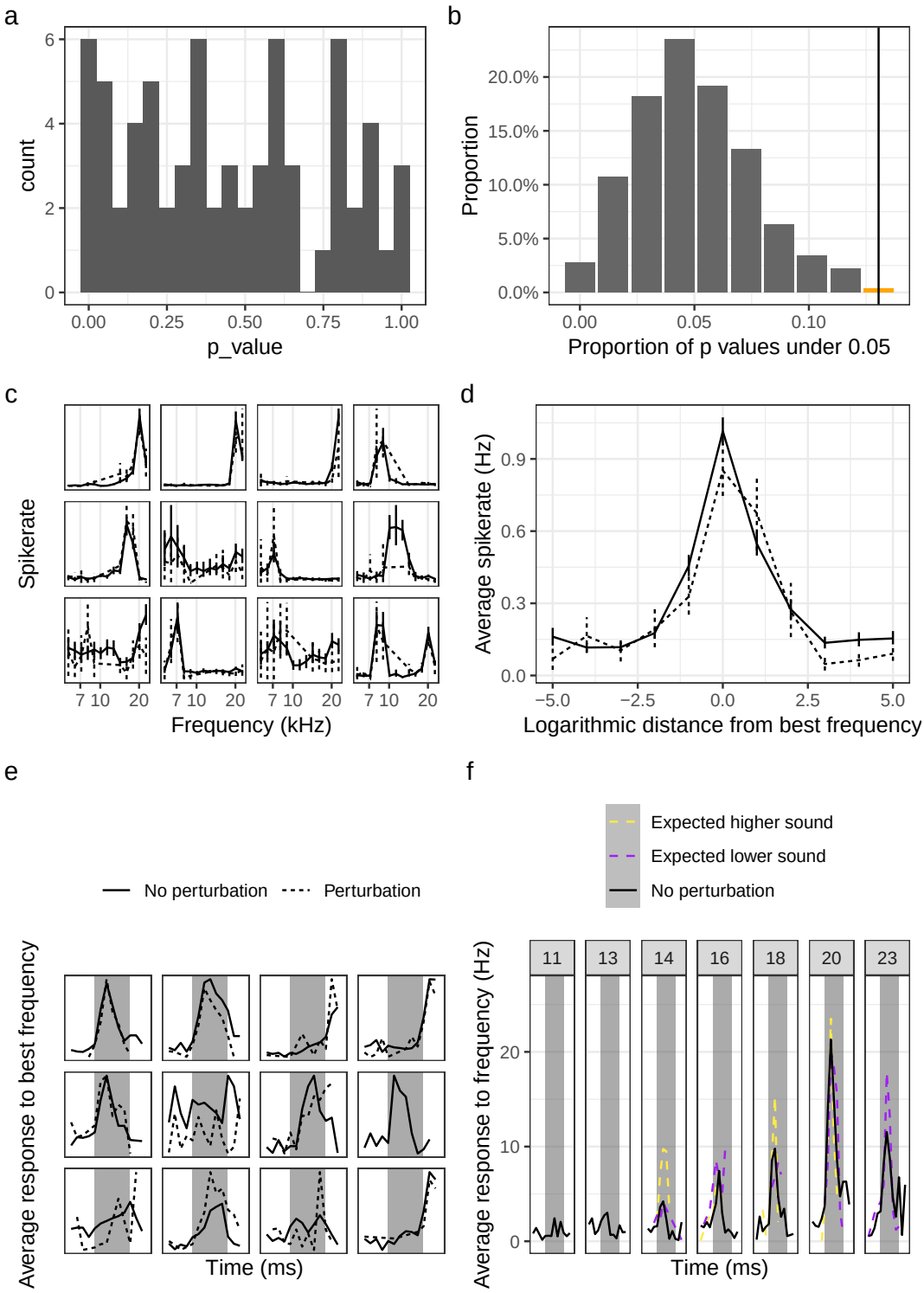

Figure 3.8: Representation of sensorimotor perturbations. **a** Distribution of the p values of the Prentice-Wittkowski test for each neuron. **b** Simulated distribution of proportions of p values under 0.05 if all underlying hypotheses were wrong. The proportion of p values under 0.05 in the given hypothesis test (marked in orange) is significantly higher than the null distribution. **c** Frequency tuning curves to perturbations and non-perturbations of neurons that are possibly sensitive to sensorimotor perturbations. **d** Average tuning curve around the best frequency for perturbations and no perturbations. **e** Average evoked response of the neurons from panel c, with and without perturbations. **f** Tuning curve of an example neuron.

4 | Discussion

In this dissertation, mice were trained on a novel sensorimotor task relating their licking behaviour to continuous auditory feedback. This dissertation focussed on analysing the acquired behavioural data, and the cortical representation in mouse M10 during one day of imaging. These data demonstrate that five out of nine analysed mice (including M10) learned the sensorimotor contingency and they suggest that the contingency was represented by neurons of the primary auditory cortex.

4.1 Behavioural evidence for task acquisition

In the novel behavioural task, the mouse could manipulate the frequency of the presented tone sequence by licking one of two spouts. They were rewarded with a small drop of water if they moved the stimulus into a particular frequency region. At any given time, the spout the animal should lick was therefore determined by the presented stimulus.

Mouse M10 reacted to the presented stimuli by increasing its lickrate in the corresponding direction. Due to the continuous integration between motor behaviour and subsequent stimulus presentation, however, a motor-driven policy (i.e. switching every few seconds between left and right lick bouts) would allow the animal to receive plenty of rewards under the regular contingency. The resulting behavioural pattern would be indistinguishable from a behavioural pattern emerging from a sound-driven policy. Whereas the reaction of M10 to the normal paradigm was therefore a necessary condition for a sound-driven policy, it was not sufficient evidence.

Importantly, this analysis suggests that the policy was at least in part driven by the presented stimuli. It might, however, also have included a learned motor pattern.

The analysis does not allow for a distinction between two alternative sound-driven policies. On the one hand, the data could be explained by an associative mechanism whereby the animal learned to lick into a certain direction as a response to the presented sounds, but did not take into account how this

licking behaviour changed this stimulus presentation. On the other hand, an integrated mechanism would propose that the animal learned to navigate in a one-dimensional tonespace using left and right licks, and used this rule to reach a rewarded frequency region. The manner in which the task was constructed aimed to make the implementation of an integrated (rather than associative) sound-driven policy more likely. In particular, this was the reason why the contingency was not presented in a trial-based manner, as this would have led the animal to focus on purely learning a behavioural response to a presented stimulus. In contrast, the continuous task approach allowed the animal to move freely in this integrated virtual environment, and to be in near-complete control of its sensory feedback. How the two sound-driven policies could be distinguished using both acquired data and further variations of the experiment will be discussed below.

4.2 Auditory cortex represents the artificial sensorimotor contingency

Sensory cortex has been found to change its tuning properties in accordance with task demands, allowing for enhanced perceptual discrimination as well as qualitative changes in the representation of task-related stimuli (Jeanne et al., 2013; Peron et al., 2015; Chu et al., 2016). In order to investigate the role of sensory areas of the cortex in task acquisition, we recorded from neurons in auditory cortex of mice while they were engaged in the task. In this dissertation, one example session in M10 was analysed.

Neurons in auditory cortex encode a reduced representation of stimulus history (Rubin et al., 2016). In order to control for this effect regular stimuli were compared to contingency violations that were otherwise fully matched in recent sensory statistics. On a population level, the representation of these sounds was significantly different. Single-neuron analysis revealed that this effect was driven by a strong difference in the responses of a small proportion of recorded neurons.

Furthermore, the analysis suggested possible mechanisms by which this representation might operate. In particular, the tuning curves derived from perturbed sounds appeared broader than the regular tuning curves. This is consistent with a model where certain neurons represent a mixture of expected and presented sounds, shifting their responses away from the presented sounds in the event of an unexpected event. In particular, one example neuron exhibited exactly this kind of pattern: Compared to its best-frequency it fired more strongly in response to a perturbation leading to a lower-frequency stimulus if the expected sound was higher and vice versa.

A clearer picture of these representational patterns will be determined using further imaging data. With a larger sample size, it would for example be possible to estimate a mathematical model of how neurons in auditory cortex represent quantities related to the sensorimotor contingency such as expected frequency and prediction error.

4.3 Implications of the behavioural and neural analysis

Combined, behavioural and neuronal evidence suggests that it is possible to train head fixed mice on a behavioural task that is based on an artificial sensorimotor contingency, leading to a cortical representation of this contingency. From a computational perspective, such a task has important implications for general theories of sensorimotor learning and intelligence. Methodologically, the fact that this computationally rich task can be applied to head fixed mice means that its neural correlates can easily be studied using 2-photon imaging and other techniques that currently cannot be applied to freely moving animals.

As a next step, the behavioural data in the other animals will be analysed to determine whether they have learned the task. Furthermore, the representation of the contingency and the manner in which sensory and motor evidence are integrated will be investigated within the available neuronal dataset. Below, I will elaborate on how the collected data can be used for such investigations and propose extensions of the task paradigm that would shed light on questions that are currently not within reach.

In computational theories of intelligence, solving more complex tasks often involves a tradeoff between two important principles of learning.

On the one hand, by extracting statistical patterns from our environment, we learn about the information we should take into account to solve these tasks. This applies to sensory statistics as well as sensorimotor contingencies. The general smoothness of objects can be used to parse information at subneuronal (Srinivasan et al., 1982) and neuronal level (Rao and Ballard, 1999). This representation is apparent in all sensory modalities (Fox and Wong, 2005; Smith and Lewicki, 2006) and is sensitive to artificial manipulations of sensory statistics (Wood, 2016; Wood and Wood, 2018). In a sensorimotor context, corollary discharges allow for sensory consequences of motor behaviour to be cancelled out. This is mediated, in part, by auditory cortex (Schneider et al., 2014) and is sensitive to artificial contingencies, as well (Schneider et al., 2018).

On the other hand, the ultimate goal of neuronal processes is to generate appropriate behaviour. Following this perspective, the brain should gradually discard task-irrelevant information to optimize

behavioural output. This idea is reflected in receptive fields in sensory cortex (Hubel and Wiesel, 1965, 1968; Aertsen et al., 1980, 1981), which can reshape their properties according to task-relevance (Fritz et al., 2003), and extends to more complex tasks such as object recognition in the ventral stream (DiCarlo et al., 2012) and semantic development in humans (Saxe et al., 2019).

The presented task lies at the interface of these two theories. On the one hand, the goal of the task is ultimately to receive a reward in the form of water. On the other hand, this goal can more easily be reached by recognizing the sensorimotor contingency. Since neural data suggests that auditory cortex represents this contingency and this area is also involved in shaping behavioural learning, it appears likely that the animal's behaviour is indeed not only driven by auditory associations, but in particular implements a contingency-driven behavioural policy.

Whether behavioural relevance has an impact on the extraction of sensorimotor contingencies in sensory cortex could be probed by making the rewards only contingent on the number of licks, leading the mice to explore the tonespace in any direction, without direct consequences on the likelihood of reward. This would connect the experiment more closely with the passive presentation of a novel sensorimotor contingency by Schneider et al. (2018).

Neurons that are sensitive to pure sensorimotor perturbations are likely implicated in the integration of sensory and motor evidence. Both multisensory and sensorimotor integration processes in the brain are compatible with a Bayesian model and take the uncertainty associated with the different stimuli into account (Wolpert et al., 1995; Körding et al., 2004; Körding and Wolpert, 2004; O'Reilly et al., 2012). In order to test whether the contingency representation in auditory cortex was implicated in a similar mechanism of evidence integration, the sound levels were modulated on some sessions so as to present stimuli with different degrees of uncertainty. These level modulations can be used to probe the purpose of the perturbation-sensitive neurons. As an example, if the neuron in figure 3.8b indeed represents a mixture of the presented and expected sound, the neuron's tuning curve would be shifted closer to the expected rather than the presented sound for less certain, i. e. more silent auditory input. Extensions of this idea might manipulate precision of the auditory stimuli by increasing their bandwidth or presenting several stimuli at once.

Similarly to the neuronal representation, the existence of an internal model can be tested behaviourally by manipulating the precision of the provided information (Wolpert et al., 1995). This would allow for a behavioural examination of whether the mice take the sensorimotor contingency into account when solving the task. The neural evidence of a representation of the contingency in auditory cortex, an area that plays a role in behavioural learning, would suggest that this contingency can affect the mouse's behaviour as well.

When freely moving rats were presented with a similar tonespace, recordings of the entorhinal-hippocampal circuit provided evidence for the emergence of grid cells representing this tonespace (Aronov et al., 2017). Grid cells had initially been identified as a neural correlate of invariant spatial behaviour (Hafting et al., 2005). More recently, they have also been implicated in non-spatial cognitive tasks (Constantinescu et al., 2016), which provides support for the hypothesis that conceptual knowledge is organized in 'cognitive maps' (Tolman, 1948). The emergence of grid cells in this behavioural task could be tested by determining the anatomical connections of the neurons representing sensorimotor perturbations and subsequently imaging entorhinal cortex in behaving mice (Low et al., 2014). Furthermore, grid cells generate a particularly precise error-correcting code compared to classical population codes in sensory cortex (Sreenivasan and Fiete, 2011). A better understanding of the representation of sensorimotor perturbations, which require such an error correction, might therefore shed light on the emergence of conceptual grid cells as well.

For the purpose of dissecting the circuit mediating this potential contingency representation, it would also be important to image inhibitory neurons in auditory cortex, as the proposed mechanism would involve cancelling out predictions from another cortical area (Larkum et al., 1999).

In conclusion, this dissertation presented a new behavioural task for head-fixed mice involving the learning of a novel, continuous auditory sensorimotor contingency. Mice were able to learn this task, and neural data suggest that auditory cortex can represent the corresponding contingency. As a next step, the variations in the collected data will allow for a more detailed examination of the implemented behavioural policy, the representation of the contingency, and the manner by which the sensory and motor evidence is integrated to guide behaviour. Furthermore, variations of the task would allow for an examination of the influence of behavioural relevance on the possible emergence of an abstract tonespace, connecting a simple task in head fixed mice to some of the most debated computational theories of learning.

Appendix

A | Licking behavior of all mice

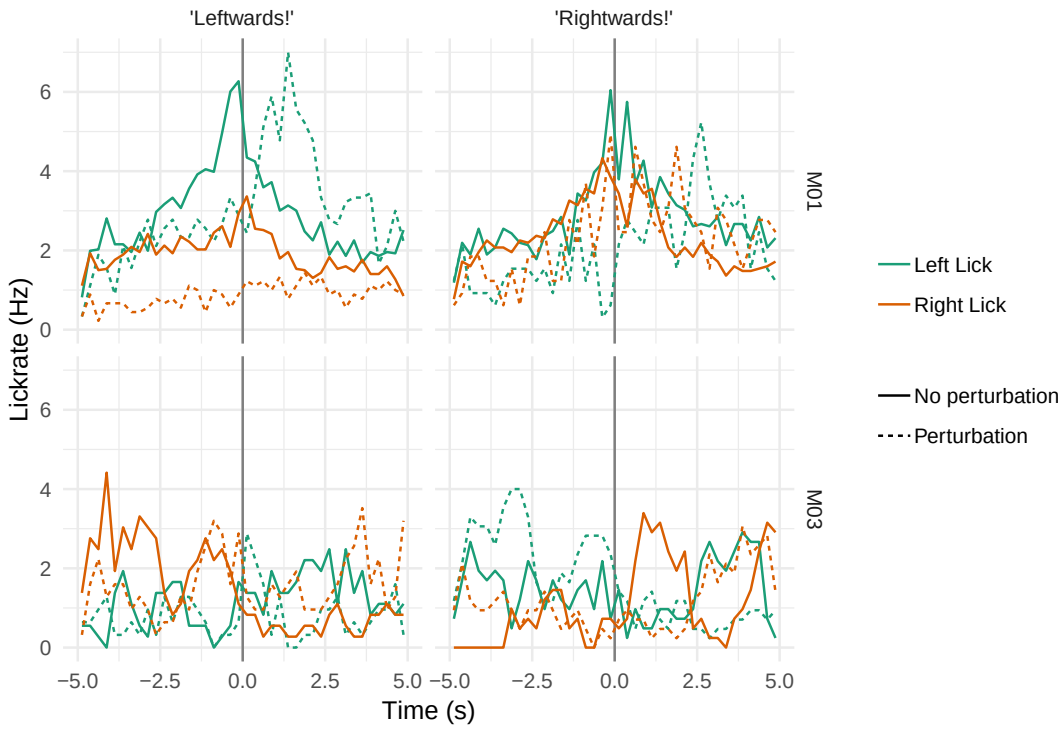

Figure A.1: Reaction of M01 and M03 to strategy perturbations

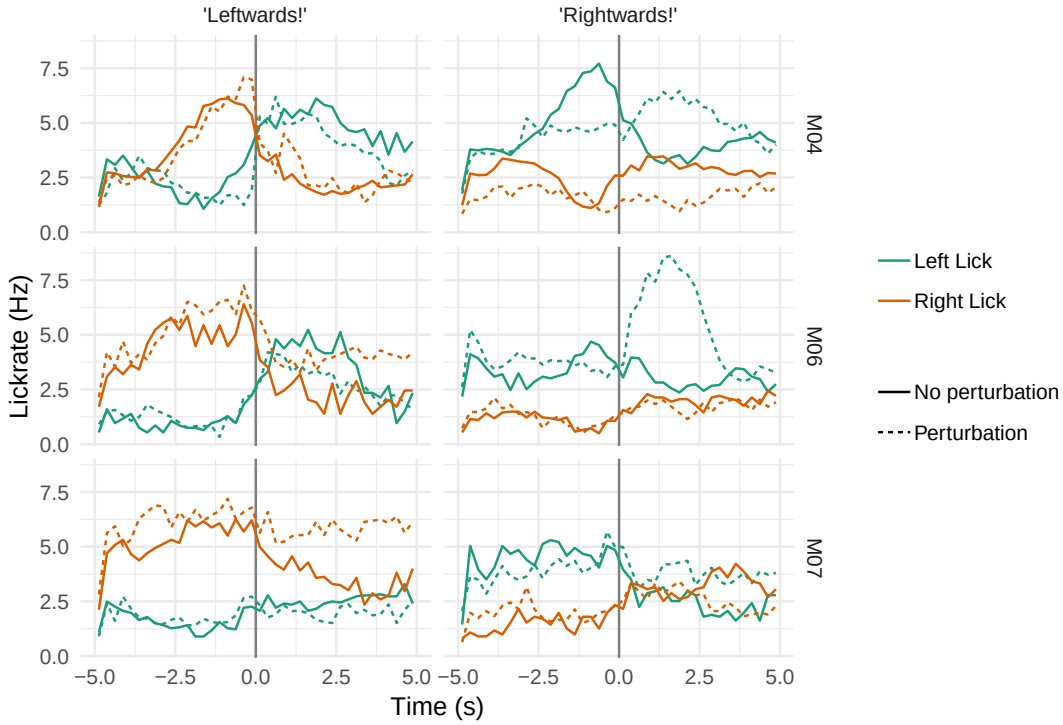

Figure A.2: Reaction of M04, M06, and M07 to strategy perturbations

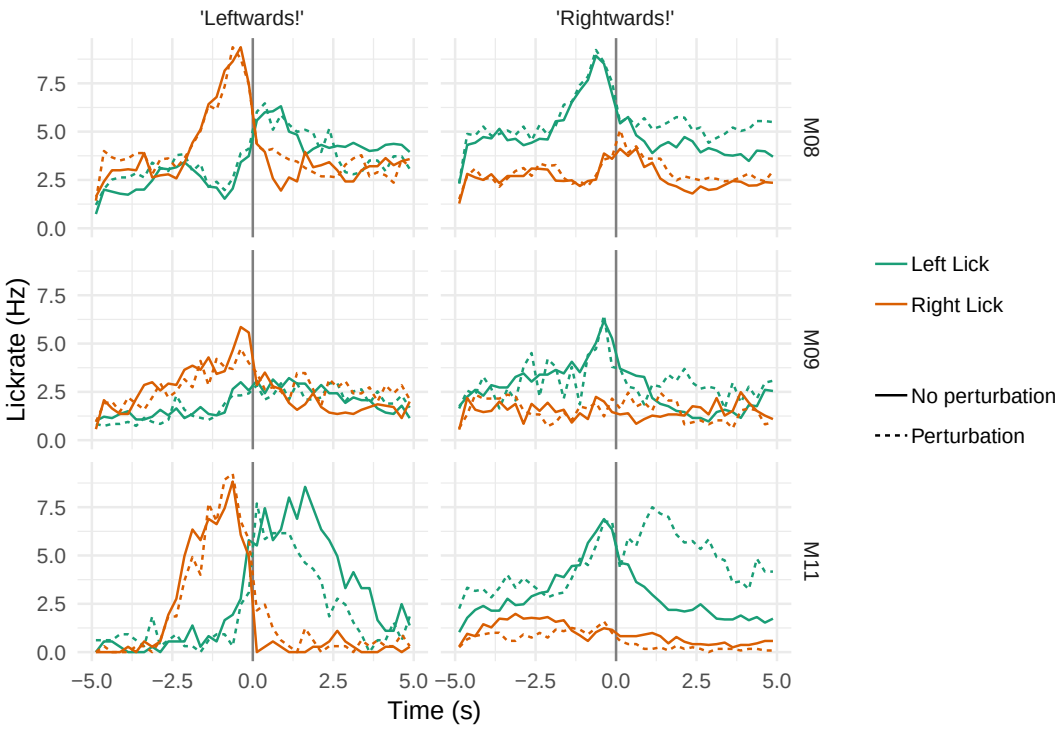

Figure A.3: Reaction of M08, M09, and M11 to strategy perturbations

Bibliography

Aertsen, A. M., Olders, J. H., and Johannesma, P. I. (1981). Spectro-temporal receptive fields of auditory neurons in the grassfrog. III. Analysis of the stimulus-event relation for natural stimuli. *Biological cybernetics*, 39(3):195–209.

Aertsen, A. M. H. J., Johannesma, P. I. M., and Hermes, D. J. (1980). Spectro-temporal receptive fields of auditory neurons in the grassfrog. *Biological Cybernetics*, 38(4):235–248.

Allaire, J., Xie, Y., McPherson, J., Luraschi, J., Ushey, K., Atkins, A., Wickham, H., Cheng, J., Chang, W., and Iannone, R. (2019). *rmarkdown: Dynamic Documents for R.* R package version 1.14.

Aronov, D., Nevers, R., and Tank, D. W. (2017). Mapping of a non-spatial dimension by the hippocampal–entorhinal circuit. *Nature*, 543(7647):719–722.

Bache, S. M. and Wickham, H. (2014). *magrittr: A Forward-Pipe Operator for R.* R package version 1.5.

Behrens, T. E. J., Woolrich, M. W., Walton, M. E., and Rushworth, M. F. S. (2007). Learning the value of information in an uncertain world. *Nature Neuroscience*, 10(9):1214–1221.

Berkes, P., Orbán, G., Lengyel, M., and Fiser, J. (2011). Spontaneous cortical activity reveals hallmarks of an optimal internal model of the environment. *Science*.

Bizley, J. K., Nodal, F. R., Nelken, I., and King, A. J. (2005). Functional Organization of Ferret Auditory Cortex. *Cerebral Cortex*, 15(10):1637–1653.

Brainard, D. H. (1997). The Psychophysics Toolbox. *Spatial Vision*, 10:433–436.

Chen, T.-W., Wardill, T. J., Sun, Y., Pulver, S. R., Renninger, S. L., Baohan, A., Schreiter, E. R., Kerr, R. A., Orger, M. B., Jayaraman, V., Looger, L. L., Svoboda, K., and Kim, D. S. (2013). Ultrasensitive fluorescent proteins for imaging neuronal activity. *Nature*, 499(7458):295–300.

Chu, M. W., Li, W. L., and Komiyama, T. (2016). Balancing the robustness and efficiency of odor representations during learning. *Neuron*, 92(1):174–186.

Constantinescu, A. O., O'Reilly, J. X., and Behrens, T. E. J. (2016). Organizing conceptual knowledge in humans with a gridlike code. *Science (New York, N.Y.)*, 352(6292):1464–1468.

DiCarlo, J. J., Zoccolan, D., and Rust, N. C. (2012). How does the brain solve visual object recognition? *Neuron*, 73(3):415–434.

Eliades, S. J. and Tsunada, J. (2018). Auditory cortical activity drives feedback-dependent vocal control in marmosets. *Nature Communications*, 9(1):2540.

Ernst, M. O. and Banks, M. S. (2002). Humans integrate visual and haptic information in a statistically optimal fashion. *Nature*, 415(6870):429–433.

Fox, K. and Wong, R. O. L. (2005). A comparison of experience-dependent plasticity in the visual and somatosensory systems. *Neuron*, 48(3):465–477.

Fritz, J., Shamma, S., Elhilali, M., and Klein, D. (2003). Rapid task-related plasticity of spectrotemporal receptive fields in primary auditory cortex. *Nature Neuroscience*, 6(11):1216–1223.

Gallistel, C. R., Mark, T. A., King, A. P., and Latham, P. E. (2001). The rat approximates an ideal detector of changes in rates of reward: Implications for the law of effect. *Journal of Experimental Psychology: Animal Behavior Processes*, 27(4):354–372.

Gill, P., Woolley, S. M. N., Fremouw, T., and Theunissen, F. E. (2008). What's That Sound? Auditory Area CLM Encodes Stimulus Surprise, Not Intensity or Intensity Changes. *Journal of Neurophysiology*, 99(6):2809–2820.

Guizar-Sicairos, M., Thurman, S. T., and Fienup, J. R. (2008). Efficient subpixel image registration algorithms. *Opt. Lett.*, 33(2):156–158.

Hafting, T., Fyhn, M., Molden, S., Moser, M.-B., and Moser, E. I. (2005). Microstructure of a spatial map in the entorhinal cortex. *Nature*, 436(7052):801–806.

Hodges, J. L. and Lehmann, E. L. (1956). The Efficiency of Some Nonparametric Competitors of the t-Test. *The Annals of Mathematical Statistics*, 27(2):324–335.

Hubel, D. H. and Wiesel, T. N. (1965). Receptive Fields and Functional Architecture in Two Nonstriate Visual Areas (18 and 19) of the Cat. *Journal of neurophysiology*, 28:229–89.

Hubel, D. H. and Wiesel, T. N. (1968). Receptive fields and functional architecture of monkey striate cortex. *The Journal of Physiology*, 195(1):215–243.

Issa, J. B., Haeffele, B. D., Agarwal, A., Bergles, D. E., Young, E. D., and Yue, D. T. (2014). Multiscale Optical Ca2+ Imaging of Tonal Organization in Mouse Auditory Cortex. *Neuron*, 83(4):944–959.

Jeanne, J. M., Sharpee, T. O., and Gentner, T. Q. (2013). Associative learning enhances population coding by inverting interneuronal correlation patterns. *Neuron*, 78(2):352–63.

Jones, E., Oliphant, T., Peterson, P., and Others (2019). SciPy: Open source scientific tools for Python.

Keller, G. B., Bonhoeffer, T., and Hübener, M. (2012). Sensorimotor Mismatch Signals in Primary Visual Cortex of the Behaving Mouse. *Neuron*, 74(5):809–815.

Kleiner, M., Brainard, D. H., and Pelli, D. G. (2007). "What's new in Psychtoolbox-3?". *Perception*, 36.

Körding, K. P., Ku, S.-p., and Wolpert, D. M. (2004). Bayesian Integration in Force Estimation. *Journal of Neurophysiology*, 92(5):3161–3165.

Körding, K. P. and Wolpert, D. M. (2004). Bayesian integration in sensorimotor learning. *Nature*, 427(6971):244–247.

Kruskal, W. H. and Wallis, W. A. (1952). Use of Ranks in One-Criterion Variance Analysis. *Journal of the American Statistical Association*, 47(260):583–621.

Larkum, M. E., Zhu, J. J., and Sakmann, B. (1999). A new cellular mechanism for coupling inputs arriving at different cortical layers. *Nature*, 398(6725):338–341.

Leinweber, M., Ward, D. R., Sobczak, J. M., Attinger, A., and Keller, G. B. (2017). A Sensorimotor Circuit in Mouse Cortex for Visual Flow Predictions. *Neuron*, 95(6):1420–1432.

Liu, J., Whiteway, M. R., Sheikhattar, A., Butts, D. A., Babadi, B., and Kanold, P. O. (2019). Parallel Processing of Sound Dynamics across Mouse Auditory Cortex via Spatially Patterned Thalamic Inputs and Distinct Areal Intracortical Circuits. *Cell Reports*, 27(3):872–885.e7.

Low, R. J., Gu, Y., and Tank, D. W. (2014). Cellular resolution optical access to brain regions in fissures: imaging medial prefrontal cortex and grid cells in entorhinal cortex. *Proceedings of the National Academy of Sciences of the United States of America*, 111(52):18739–44.

McKinney, W. (2010). Data Structures for Statistical Computing in Python.

Miall, R. C. and Wolpert, D. M. (1996). Forward Models for Physiological Motor Control. *Neural Networks*, 9(8):1265–1279.

Oliphant, T. E. (2006). *Guide to NumPy*.

O'Reilly, J. X., Jbabdi, S., and Behrens, T. E. J. (2012). How can a Bayesian approach inform neuroscience? *European Journal of Neuroscience*, 35(7):1169–1179.

Pachitariu, M., Stringer, C., Schröder, S., Dipoppa, M., Rossi, L. F., Carandini, M., and Harris, K. D. (2017). Suite2p: beyond 10,000 neurons with standard two-photon microscopy. *bioRxiv*.

Pelli, D. G. (1997). The VideoToolbox software for visual psychophysics: Transforming numbers into movies. *Spatial Vision*, 10:437–442.

Peron, S. P., Freeman, J., Iyer, V., Guo, C., and Svoboda, K. (2015). A Cellular Resolution Map of Barrel Cortex Activity during Tactile Behavior. *Neuron*, 86(3):783–799.

Poulet, J. F. A. and Hedwig, B. (2003). Corollary discharge inhibition of ascending auditory neurons in the stridulating cricket. *The Journal of neuroscience : the official journal of the Society for Neuroscience*, 23(11):4717–25.

Prentice, R. L. and Pyke, R. (1979). Logistic disease incidence models and case-control studies. *Biometrika*, 66(3):403–411.

Qin, L., Chimoto, S., Sakai, M., Wang, J., and Sato, Y. (2007). Comparison Between Offset and Onset Responses of Primary Auditory Cortex on – off Neurons in Awake Cats. *Journal of Neurophysiology*, 97(5):3421–3431.

R Core Team (2018). *R: A Language and Environment for Statistical Computing*. R Foundation for Statistical Computing, Vienna, Austria.

Rao, R. P. N. and Ballard, D. H. (1999). Predictive coding in the visual cortex: a functional interpretation of some extra-classical receptive-field effects. *Nature Neuroscience*, 2(1):79–87.

Robinson, D. and Hayes, A. (2018). *broom: Convert Statistical Analysis Objects into Tidy Tibbles*. R package version 0.5.0.

Rossum, G. (1995). Python reference manual.

Rubin, J., Ulanovsky, N., Nelken, I., and Tishby, N. (2016). The Representation of Prediction Error in Auditory Cortex. *PLoS Computational Biology*, 12(8):1–28.

Saxe, A. M., McClelland, J. L., and Ganguli, S. (2019). A mathematical theory of semantic development in deep neural networks. *Proceedings of the National Academy of Sciences of the United States of America*, 116(23):11537–11546.

Schneider, D. M., Nelson, A., and Mooney, R. (2014). A synaptic and circuit basis for corollary discharge in the auditory cortex. *Nature*, 513(7517):189–194.

Schneider, D. M., Sundararajan, J., and Mooney, R. (2018). A cortical filter that learns to suppress the acoustic consequences of movement. *Nature*, 561(7723):391–395.

Slotnick, B. (2009). A Simple 2-Transistor Touch or Lick Detector Circuit. *Journal of the Experimental Analysis of Behavior*, 91(2):253–255.

Smith, E. C. and Lewicki, M. S. (2006). Efficient auditory coding. *Nature*, 439(7079):978.

Spinu, V., Grolemund, G., and Wickham, H. (2018). *lubridate: Make Dealing with Dates a Little Easier*. R package version 1.7.4.

Sreenivasan, S. and Fiete, I. (2011). Grid cells generate an analog error-correcting code for singularly precise neural computation. *Nature Neuroscience*, 14(10):1330–1337.

Srinivasan, M. V., Laughlin, S. B., and Dubs, A. (1982). Predictive Coding: A Fresh View of Inhibition in the Retina. *Proceedings of the Royal Society of London. Series B, Biological Sciences*, 216(1205):427–459.

Stiebler, I., Neulist, R., Fichtel, I., and Ehret, G. (1997). The auditory cortex of the house mouse: left-right differences, tonotopic organization and quantitative analysis of frequency representation. *Journal of Comparative Physiology A: Sensory, Neural, and Behavioral Physiology*, 181(6):559–571.

Tolman, E. C. (1948). Cognitive maps in rats and men. *Psychological review*, 55(4):189–208.

Urbanek, S. (2013). *png: Read and write PNG images*. R package version 0.1-7.

Ushey, K., Allaire, J., and Tang, Y. (2019). *reticulate: Interface to 'Python'*. R package version 1.12.

van der Walt, S., Colbert, S. C., and Varoquaux, G. (2011). The NumPy Array: A Structure for Efficient Numerical Computation. *Computing in Science & Engineering*, 13(2):22–30.

Weissenberger, Y., King, A. J., and Dahmen, J. C. (2019). Decoding mouse behavior to explain single-trial decisions and their relationship with neural activity. *bioRxiv*.

Westerman, L. A. and Smith, R. L. (1984). Rapid and short-term adaptation in auditory nerve responses. *Hearing Research*, 15(3):249–260.

Wickham, H. (2019a). *feather: R Bindings to the Feather 'API'*. R package version 0.3.3.

Wickham, H. (2019b). *stringr: Simple, Consistent Wrappers for Common String Operations*. R package version 1.4.0.

Wickham, H., Chang, W., Henry, L., Pedersen, T. L., Takahashi, K., Wilke, C., and Woo, K. (2019a). *ggplot2: Create Elegant Data Visualisations Using the Grammar of Graphics*. R package version 3.1.1.

Wickham, H., François, R., Henry, L., and Müller, K. (2019b). *dplyr: A Grammar of Data Manipulation*. R package version 0.8.0.1.

Wickham, H. and Henry, L. (2018). *tidyr: Easily Tidy Data with 'spread()' and 'gather()' Functions*. R package version 0.8.1.

Wittkowski, K. M. (2007). Small Sample Properties of Rank Tests for Incomplete Unbalanced Designs. *Biometrical Journal*, 30(7):799–808.

Wittkowski, K. M. and Song, T. (2012). *muStat: Prentice Rank Sum Test and McNemar Test*. R package version 1.7.0.

Wolpert, D., Ghahramani, Z., and Jordan, M. (1995). An internal model for sensorimotor integration. *Science*, 269(5232):1880–1882.

Wood, J. N. (2016). A smoothness constraint on the development of object recognition. *Cognition*, 153:140–145.

Wood, J. N. and Wood, S. M. (2018). The Development of Invariant Object Recognition Requires Visual Experience With Temporally Smooth Objects. *Cognitive Science*, 42(4):1391–1406.

Xie, Y. (2018). *bookdown: Authoring Books and Technical Documents with R Markdown*. R package version 0.7.

Xie, Y. (2019). *knitr: A General-Purpose Package for Dynamic Report Generation in R*. R package version 1.23.